Diffusion in periodic potentials with path integral hyperdynamics

T. Ikonen,[1] M. D. Khandkar,[1,2] L. Y. Chen,[3] S. C. Ying,[4] and T. Ala-Nissila[1,4]

[1]*Department of Applied Physics and Centre of Excellence in Computational Nanoscience (COMP), Aalto University School of Science, P.O. Box 11000, FI-00076 Aalto, Espoo, Finland*
[2]*Department of Applied Sciences, Pillai's Institute of Information Technology (PIIT), Sector 16, New Panvel 410206, India*
[3]*Department of Physics, University of Texas at San Antonio, San Antonio, Texas 78249-0697, USA*
[4]*Department of Physics, Brown University, Providence, Rhode Island 02912-1843, USA*

We consider the diffusion of Brownian particles in one-dimensional periodic potentials as a test bench for the recently proposed stochastic path integral hyperdynamics (PIHD) scheme [Chen and Horing, J. Chem. Phys. **126**, 224103 (2007)]. First, we consider the case where PIHD is used to enhance the transition rate of activated rare events. To this end, we study the diffusion of a single Brownian particle moving in a spatially periodic potential in the high-friction limit at low temperature. We demonstrate that the boost factor as compared to straight molecular dynamics (MD) has nontrivial behavior as a function of the bias force. Instead of growing monotonically with the bias, the boost attains an optimal maximum value due to increased error in the finite path sampling induced by the bias. We also observe that the PIHD method can be sensitive to the choice of numerical integration algorithm. As the second case, we consider parallel resampling of multiple bias force values in the case of a Brownian particle in a periodic potential subject to an external ac driving force. We confirm that there is no stochastic resonance in this system. However, while the PIHD method allows one to obtain data for multiple values of the ac bias, the boost with respect to MD remains modest due to the simplicity of the equation of motion in this case.

I. INTRODUCTION

The study of particles performing Brownian motion in a periodic potential constitutes a hallmark example of stochastic particle dynamics with important applications in various branches of science and technology. Perhaps the most common application of periodic Brownian motion is the diffusive dynamics of atoms and molecules on crystal surfaces [1]. Surface diffusion is among the most important mechanisms that control processes such as island nucleation and subsequent surface growth. It has been shown that controlling the mobility of particles on the surface by external means, such as an ac or dc electric field, allows morphological control over the growing surfaces [1]. It is thus of great interest to model periodic Brownian motion with static and time-dependent external fields.

To this end, there have been several studies reporting the diffusion of a single Brownian particle in a periodic potential with external ac bias applied [2–5]. Most of the studies reporting the behavior of Brownian particles discuss the influence of an oscillating bias on transport coefficients. The central issue here is the existence of a stochastic resonance (SR), which can greatly enhance the diffusion coefficient D in two dimensions [3]. However, it has been shown in the case of one-dimensional (1D) periodic potentials that although the local jump rate of particles can be enhanced, there is no true SR in the hydrodynamic limit [2,5].

An interesting limit of the periodic Brownian motion is where the energy barrier V_0 is much larger than the thermal energy (i.e., $\beta V_0 \gg 1$ [1], where $\beta = 1/k_B T$, k_B is the Boltzmann constant, and T the absolute temperature). Since Brownian motion is activated by thermal fluctuations, the diffusion rate is proportional to $\exp(-\beta V_0)$, which becomes very small at low temperatures. To overcome this rare event

problem in molecular dynamics (MD) simulations, Voter [6] has proposed the so-called hyperdynamics (HD) scheme, which involves accelerating the dynamics by adding proper bias potential, which effectively lowers the barrier height. The dynamics is then corrected based on the approximate transition state theory (TST). There exist various approaches to the choice of the bias potential, and some examples can be found in Refs. [7–10].

However, a scheme has been proposed that is based on the mapping of the stochastic Langevin equation to a path integral form [11]. Unlike the standard HD scheme, this so-called stochastic path integral hyperdynamics (PIHD) method allows an exact correction of the dynamics by resampling the simulated paths. In other words, this method is not restricted to the TST approximation. Further, it is not restricted to static energy barriers; both entropic barriers and even time-dependent bias can be employed. This allows an efficient way to overcome the large barrier problem, as demonstrated in Ref. [11]. However, a systematic study of the efficiency of the PIHD method is needed. In this work, we perform numerical studies of monomer diffusion in a one-dimensional (1D) periodic potential in the low-temperature and high-friction regime, where the analytical solution of the barrier crossing rate is known. We study the computational efficiency of the PIHD method with two different types of bias potential, revealing nonmonotonic behavior of the boost factor. We also develop a simple mathematical model that explains the observed behavior. Furthermore, the PIHD method is not limited to the case of high barriers. Since in principle any external bias force can be used, it should be possible to obtain results for many different bias values from running Langevin dynamics (LD) simulations with a single value of the bias force, or even without such a force if need be. To demonstrate this parallel resampling, we employ the PIHD method to study

the diffusion of a single Brownian particle in a 1D periodic potential with ac forcing and, show how the PIHD method can be employed to obtain the transport coefficients for a range of different external forcing terms from a single simulation run. However, in this case the boost obtained remains modest due to the simplicity of the equations of motion to be integrated.

II. PATH INTEGRAL HYPERDYNAMICS

Brownian motion of a single particle can be represented by the Langevin equation

$$m\ddot{r}(t) + m\gamma \dot{r}(t) - F = \xi(t), \tag{1}$$

where $r(t)$ denotes the position of the particle of mass m at time t, moving under the influence of external force F. The random force $\xi(t)$ satisfies $\langle \xi(t) \rangle = 0$ and $\langle \xi_i(t)\xi_j(t') \rangle = 2k_B T m\gamma \delta_{i,j}\delta(t - t')$, where γ denotes the friction coefficient, k_B is the Boltzmann constant and T is the absolute temperature. The probability density of finding the particle at r_f at t given the initial position r_0 at t_0 is

$$P(r_0, t_0 | r_f, t) = C \int [\mathrm{D}r] \exp\{-\beta \mathrm{I}[r(t)]\}, \tag{2}$$

where C is a normalization constant, $[Dr]$ represents the path integral over all possible trajectories $r(t)$, and the effective action is given by

$$I[r(t)] = \frac{1}{4m\gamma} \int_{t_0}^{t} dt'[m\ddot{r}(t') + m\gamma \dot{r}(t') - F]^2. \tag{3}$$

In a system with an energy barrier much larger than the thermal energy $k_B T$, the probability of the particle crossing the barrier is very small. To make such transition events more frequent, a bias force $F_b(r,t)$ is added to the external force F. In this boosted system, the particle obeys the Langevin equation

$$m\ddot{r}(t) + m\gamma \dot{r}(t) - F = \xi(t) + F_b(r,t). \tag{4}$$

Obviously, this leads to dynamics and transition probabilities that are different from those given by Eqs. (1) and (2). However, as demonstrated in Refs. [11–13], it is possible to exactly recover the original probability density of Eq. (2) from the biased dynamics by writing

$$P(r_0, t_0 | r_f, t) = C \int [Dr] \exp\{-\beta I_\mathrm{b}[r(t)]\} \exp\{-\beta I_\xi[r(t)]\}, \tag{5}$$

where the effective action can now be written in two parts: the action in the boosted system (I_b) and the correction

$$I_\xi(t) = \frac{1}{4m\gamma} \int_{t_0}^{t} dt' F_b[r(t'),t']\{F_b[r(t'),t'] + 2\xi(t')\}. \tag{6}$$

In the end-point (Ito) discretization scheme this integral reduces to the discrete sum

$$I_\xi(t) = \frac{1}{4m\gamma} \sum_i F_b(r,t_i) [F_b(r,t_i) + 2\xi(t_i)] \Delta t. \tag{7}$$

To recover true dynamics in the absence of $F_b(r,t)$, one has to estimate the PIHD statistical weight factor $\exp(-\beta I_\xi)$ and simply use it to reweight every sampled trajectory. Here, the

trajectories are sampled over all dynamical paths $r(t)$ starting from a pretransition state A ($x_A < x_c$) at time t_0 to state B located at $x_B > x_c$ at time t, where x_c represents a certain transition state. The transition probability $p(t)$ from state A to state B is given by the relation

$$p(t) = \int_{x_f \geqslant x_c} dr_f \int_{x_0 \leqslant x_c} dr_0 P(r_0) P(r_0, t_0 | r_f, t). \tag{8}$$

Here, the integrals are calculated over all accessible post-transition and all pretransition states given by the initial quasiequilibrium distribution $P(r_0)$ of the particle in the unbiased system.

III. DIFFUSION IN PERIODIC POTENTIAL

The fundamental quantity associated with Brownian dynamics is the single-particle (tracer) diffusion coefficient [1], which in one dimension can be defined through the mean square displacement (MSD) of the tracer particle as

$$D = \lim_{t \to \infty} \frac{1}{2t} \langle [r(t) - r(0)]^2 \rangle. \tag{9}$$

When studying particle diffusion the mean square displacement at zero bias (true dynamics) can be obtained by running PIHD with a bias force, calculating $I_\xi(t)$ along every sampled trajectory and reweighting as

$$\langle [r(t) - r(0)]_\mathrm{MD}^2 \rangle = \langle [r(t) - r(0)]_\mathrm{PIHD}^2 e^{-\beta I_\xi} \rangle, \tag{10}$$

where the subscripts MD and PIHD correspond to the quantities with zero bias (true dynamics) and finite bias, respectively.

When considering diffusion in an external, periodic potential the definition Eq. (9) of the diffusion coefficient is convenient in the regime of intermediate to low friction γ, where the particle often makes continuous jumps across multiple saddle points. In this case, it is in principle possible, but not practical, to define all the post-transition states and transition probabilities. Instead, the PIHD method can be easily applied in this regime by using Eq. (10) for the MSD. On the other hand, in the low-temperature and high-friction regime, virtually all jumps are to the nearest-neighbor minima, which naturally define the post-transition state B. In this limit, it is advantageous to define the diffusion coefficient as (see, e.g., Ref. [1]):

$$D = \tfrac{1}{2} \Gamma \lambda^2, \tag{11}$$

where Γ is the overall jump rate, and λ is the corresponding jump length. The theoretical rate in the intermediate- to high-friction regime is given by the Kramers rate [14,15]

$$\Gamma = \frac{\omega_0}{\pi} \left[\left(\frac{\gamma^2}{4\omega_0^2} + 1 \right)^{\frac{1}{2}} - \frac{\gamma}{2\omega_0} \right] e^{-\beta V_0}, \tag{12}$$

where the frequency $\omega_0 = 2\pi\sqrt{V_0/2\lambda^2 m}$. With PIHD, the jump rate can be numerically evaluated by reweighting the barrier crossing probability as

$$p(t) = \frac{1}{N} \sum_\xi c(\xi) e^{-\beta I_\xi(t)}, \tag{13}$$

where N is the number of trajectories and $c(\xi) = 1$ for $t > t_{\mathrm{cross}}$ for crossing trajectories with crossing time t_{cross}, and zero otherwise. The rate constant is then obtained as $\Gamma = dp(t)/dt$ in the linear region of $p(t)$.

IV. MODELS AND RESULTS

A. Brownian particle in periodic potential at low temperatures

Jump rate

Although the application of PIHD to speeding up barrier crossing has been demonstrated in Refs. [11,12], the quantitative efficiency of the method as compared to straight Langevin dynamics needs to be studied. The most natural way to use PIHD is to speed up the activation of rare events by applying a bias force. To this end, in this section we consider the canonical case of activated diffusion of a Brownian monomer in a periodic potential in the limit of high friction and low temperature [1]. The equation of motion for the system is given by

$$m\ddot{x}(t) + m\gamma\dot{x}(t) - F(x) = \xi(t) + F_b(x), \qquad (14)$$

Here $F(x)$ is the force due to spatially periodic potential $V(x) = -(V_0/2)[1 - \cos(2\pi x/\lambda)]$ and $F_b(x)$ is the bias force. We set scales for length as λ, energy as $k_B T$ and mass as m. The time scale is then defined as $t_0 = \lambda\sqrt{(m/k_B T)}$ and all other relevant quantities are expressed as dimensionless. The numerical values of the parameters we have used are $\lambda = 1$, $V_0 = 1$, $\gamma = 20$, $T = 0.05$, and $m = 1$. In this range, the diffusion coefficient is to very good approximation given by Eqs. (11) and (12). We use two independent numerical integration algorithms to solve the equation of motion: the Brünger-Brooks-Karplus (BBK) algorithm [16] with time step $\Delta t = 0.01$ and the Ermak algorithm [17,18] with time step $\Delta t = 0.005$ and, thereafter Eqs. (7) and (13) to recover the unbiased jump rates. The Ermak algorithm has been used previously with PIHD in Ref. [12] to study polymer escape with intermediate friction coefficient $\gamma = 0.7$ with good accuracy. In our case of high friction ($\gamma = 20$), however, the algorithm introduced a systematic error of about 15%, which could be reduced by decreasing the time step to $\Delta t = 0.0005$. The error is caused by the extreme sensitivity of the functional integral in Eq. (7) to the numerical value of the random force $\xi_i(t)$. Within the approximation of the Ermak algorithm, the random force is preintegrated with respect to time to give the random displacement and random velocity, and at high friction this approximation requires an extremely small time step in the evaluation of the functional integral. In the BBK algorithm, however, the fluctuations are written down explicitly as a random force and the problem does not occur. Consequently, in this section we present the results obtained using the BBK algorithm as the numerical integrator, for which the same time step can be used for both MD and PIHD simulations.

We have simulated the monomer with regular MD (i.e., without bias potential) and with PIHD using two different choices of bias force: the (piecewise) constant bias force $F_b(x) = f_b$ (constant) for $x < \lambda/2$ and 0 for $x \geqslant \lambda/2$, and the (spatially) sinusoidal bias force $F_b(x) = -\frac{\pi V_b}{\lambda}\sin(2\pi x/\lambda)$, for $-\lambda/2 \leqslant x \leqslant \lambda/2$, and 0 otherwise. Examples of the boosted potentials $V(x) + V_{\mathrm{bias}}(x)$ are shown in Fig. 1. For each
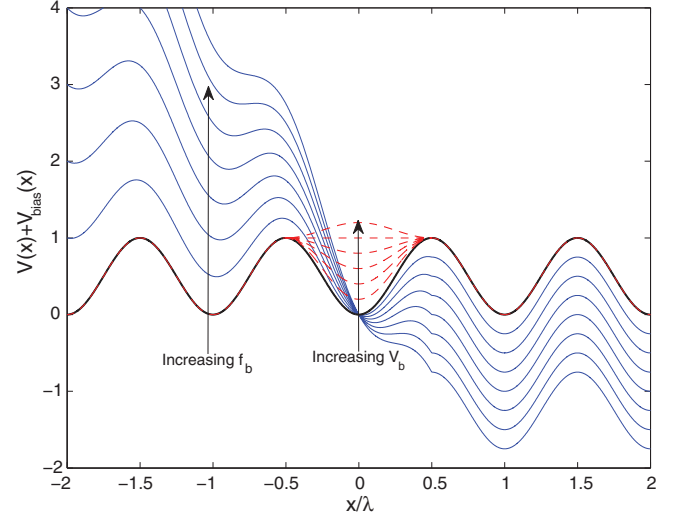

FIG. 1. (Color online) The unbiased periodic potential $V(x)$ (solid black line) and the boosted potentials for the constant bias force (solid blue line, solid gray in grayscale) and the sinusoidal bias force (dashed red line, dashed gray in grayscale) for several values of f_b and V_b. For the constant bias, the critical tilt for which the barrier height is reduced to zero, is $f_{\mathrm{cr}} = \pi$.

value of f_b (V_b) we performed simulations consisting of 10^9 independent trajectories. The initial position of the particle is sampled from the Boltzmann distribution corresponding to the unbiased external potential and, after the initial equilibration, the bias potential is switched on at time $t = 0$. Each trajectory is then simulated until the maximum simulation time $t_{\mathrm{max}} = 15$ is reached or once a successful crossing of the barrier at $x = \lambda$ occurs, at which time the value of the functional $I_\xi(t)$ is recorded. The contribution of any one crossing trajectory to the sum in Eq. (13) is therefore $\exp[-\beta I_\xi(t_{\mathrm{cross}})]$.

The results of the simulations with the constant bias force are shown in Fig. 2. Panel (a) shows the crossing probability versus time, from which the jump rate Γ is obtained as the average slope of the linear region of the curve. The $p(t)$ curves have two important features. First, the number of crossings increases steeply as the bias force is increased, resulting in a smoother curve. At the chosen temperature, the number of successful crossings with unbiased MD is in fact so low that determining the crossing rate at reasonable accuracy is not possible. In contrast, the PIHD simulations allow one to determine the rate with good accuracy. The second important feature is that the large-bias curves start to bend down after a certain time and exhibit very large jumps in $p(t)$. This behavior is the result of estimating the exponential average in Eq. (13) with a finite sample size. The finite exponential average gives large weight to the tail of the distribution of the action functional $I_\xi(t_{\mathrm{cross}})$, resulting in the occasional sudden jumps in $p(t)$ and a systematic error between the rare jumps. The error becomes larger with time because the distribution shifts toward higher values of $I_\xi(t_{\mathrm{cross}})$, making the finding of a linear slope practically impossible with very high bias forces.

In Fig. 2(b) the computed crossing rates are shown for different values of f_b. The value of Γ is determined by taking the average of $dp(t)/dt$ within the linear region of the $p(t)$ curve, which is divided into n intervals of length Δt, each
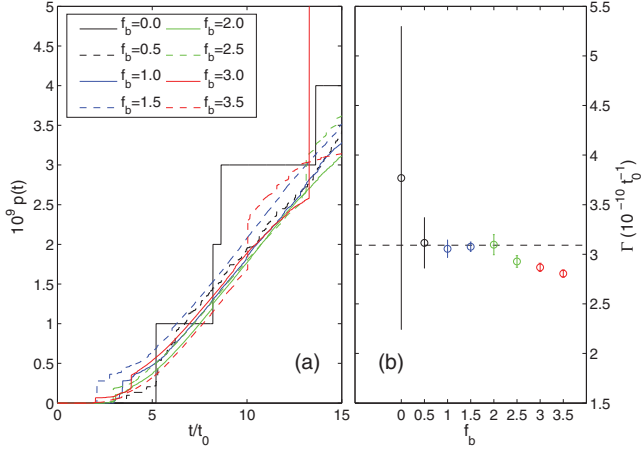
FIG. 2. (Color online) (a) The crossing probability $p(t)$ vs time t of a Brownian monomer in a sinusoidal potential well with $V_0/T = 20$. The regular MD simulations yield only four crossings out of 10^9 runs, while the PIHD simulations give several orders of magnitude more. (b) The jump rate Γ for bias force values $f_b = 0(\text{MD}), 0.5, 1.0, 1.5, 2.0, 2.5, 3.0, 3.5$. The error bars indicate the standard error of the mean value. The dashed horizontal line indicates the theoretical value at the low-temperature and high-friction limit, $\Gamma \approx 3.0919 \cdot 10^{-10}$, as calculated from Eq. (12) for one reaction pathway (the barrier to the right).

interval giving an independent value of the derivative. The standard error of Γ is calculated as $s/\sqrt{n-1}$, where s is the standard deviation of $dp(t)/dt$ within the region. The numerical values of Γ obtained with various bias forces are listed in Table I.

The corresponding results for the sinusoidal bias force are shown in Fig. 3. With the sinusoidal bias force, we also performed 10^9 independent simulation runs, using the bias amplitude V_b as the control parameter. Other parameters were the same as in the previous case of constant bias force. The results are shown in Fig. 3. Qualitatively, the results are similar to the constant bias force case, although both the systematic and statistical errors are smaller. Numerical results are shown in Table I.

TABLE I. Values of the jump rate Γ for different magnitudes f_b of the constant bias force and different amplitudes V_b of the sinusoidal bias force. The theoretical value of the jump rate is $\Gamma \approx 3.0919 \cdot 10^{-10}$.

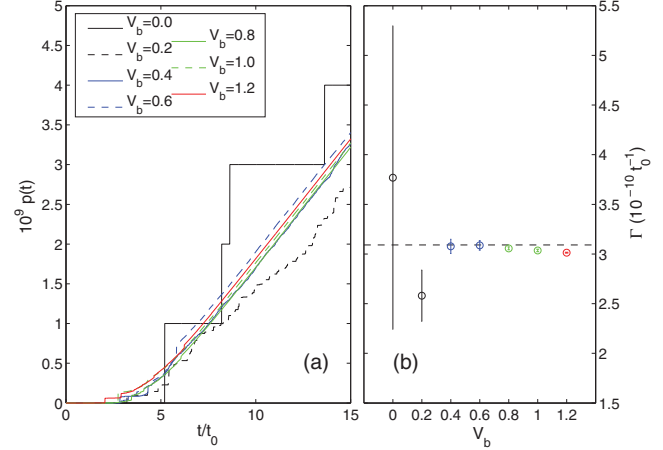| f_b	$\Gamma(10^{-10}t_0^{-1})$	V_b	$\Gamma(10^{-10}t_0^{-1})$
0.0	3.77 ± 1.53	0.0	3.77 ± 1.53
0.5	3.11 ± 0.26	0.2	2.58 ± 0.26
1.0	3.06 ± 0.09	0.4	3.08 ± 0.07
1.5	3.08 ± 0.05	0.6	3.09 ± 0.05
2.0	3.10 ± 0.10	0.8	3.06 ± 0.02
2.5	2.92 ± 0.06	1.0	3.04 ± 0.02
3.0	2.87 ± 0.04	1.2	3.01 ± 0.01
3.5	2.81 ± 0.04		

FIG. 3. (Color online) (a) The crossing probability and (b) jump rate for the sinusoidal bias force for various magnitudes of $V_b = 0, 0.2, 0.4, 0.6, 0.8, 1.0, 1.2$. Conventions are the same as in Fig. 2.

The PIHD boost factor

An important property of any hyperdynamics method is the boost factor B that describes the computational speedup due to the accelerated dynamics [6]. The simplest approach to estimating B is to consider the gain in the number of crossing paths given by the PIHD method, $g = N_{\text{PIHD}}^{\text{cross}}/N_{\text{MD}}^{\text{cross}}$. This would give the boost factor that is exponentially dependent on the decrease in barrier height. For the constant bias force, the gain is

$$g = \sqrt{1 - z^2} \exp\{\beta V_0[1 - \sqrt{1 - z^2} - z \arcsin z + z\pi/2]\},$$
(15)

where $z = \lambda f_b/\pi V_0$. This is shown in Fig. 4 as the solid black curve, along with the corresponding numerical data from simulations. However, this simple approach will give a huge overestimate of B because of the exponential average in Eq. (13). The distribution of the exponential weight factors for the crossing paths $\mathcal{P}\{\exp[-\beta I_\xi(t_{\text{cross}})]\}$ has a long tail, implying that the number of paths that give a significant contribution to the sum in Eq. (13) constitute only a small fraction of the total number of crossing paths. As a result, the actual boost factor is in reality much lower than the gain in number of crossings, especially for large bias forces.

To quantify the computational speedup given by PIHD, we define B as the ratio of computational time of conventional MD simulations over the computational time of PIHD simulations required to give the same accuracy of the crossing rate. With conventional MD, the variance of the mean is inversely proportional to the number of crossings, implying that $B = \sigma_{\text{MD}}^2/\sigma_{\text{PIHD}}^2$. However, because of the increasing systematic error with high bias, it is more appropriate to use the mean squared error (MSE) instead of the variance. The MSE for the estimator of the mean rate Γ is the sum of the variance and the square of systematic error Y (in statistics, the latter is often called estimator bias, but to avoid confusion with the hyperdynamics bias, we use the term systematic error)

$$\text{MSE}(\hat{\Gamma}) = \sigma_\Gamma^2(\hat{\Gamma}) + Y(\hat{\Gamma}, \Gamma)^2.$$
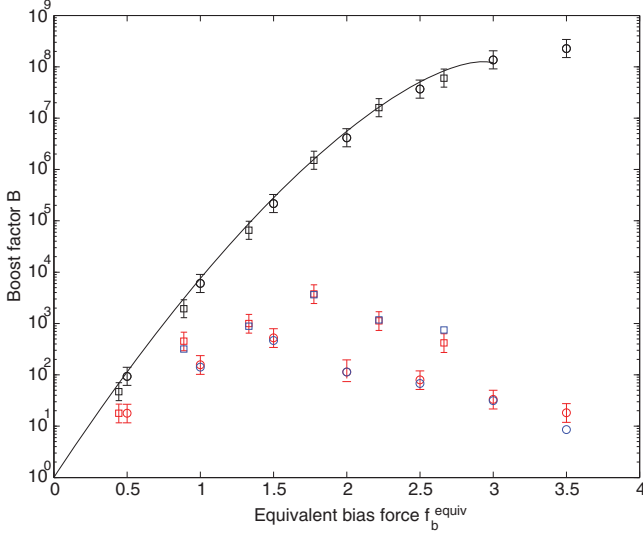(16)

FIG. 4. (Color online) The PIHD boost factor B as a function of equivalent constant bias force f_b^{equiv} for both the constant bias force (circles) and the sinusoidal force (squares). For the constant bias force, $f_b^{\text{equiv}} = f_b$, while for the sinusoidal force, $f_b^{\text{equiv}} = \frac{\pi}{\sqrt{2}} V_b$. The solid black curve indicates the theoretical gain in number of crossings given by Eq. (15), with the black markers being the corresponding values from PIHD simulations. The red (gray) markers with error bars are the boost factors measured from simulations on the basis of Eqs. (16)–(18). The blue (gray) markers without error bars show the corresponding boost factors calculated with the random deposition model from the measured distributions of $I_\xi(t_{\text{cross}})$.

We then define the boost factor as

$$B = \text{MSE}_{\text{MD}}/\text{MSE}_{\text{PIHD}}. \qquad (17)$$

While the choice of MSE as a measure of B is certainly not unique, it has the benefit of being a well-established measure of accuracy of estimators and it captures the typical behavior of biased PIHD simulations: for low to moderate bias, the MSE (and consequently, the boost) is mostly determined by the variance σ^2, but for large bias, the systematic error becomes increasingly important. We define the systematic error as

$$Y(\hat{\Gamma}, \Gamma) = \max[0, \Gamma - \hat{\Gamma} - \sigma_\Gamma(\hat{\Gamma})], \qquad (18)$$

where Γ is the theoretical value given by Eq. (12) and $\hat{\Gamma}$ and $\sigma_\Gamma(\hat{\Gamma})$ refer to the values given by the PIHD simulations. The upper limit $\hat{\Gamma} + \sigma_\Gamma(\hat{\Gamma})$ is used instead of the mean value $\hat{\Gamma}$ to avoid double counting of the statistical error.

The measured boost factor B for various levels of bias for both the constant and sinusoidal bias potentials is shown in Fig. 4. To compare the constant and sinusoidal bias potentials, the amplitude V_b of the sinusoidal force is expressed in terms of an equivalent constant bias force f_b^{equiv} by scaling the amplitude with the spatial rms average of the sinusoidal bias force, $\sqrt{\frac{1}{\lambda} \int_{-\lambda/2}^{\lambda/2} [F_b(x)]^2 dx} = \frac{\pi}{\sqrt{2}}$. In addition, the boost factor for the constant bias force given by Eqs. (16)–(18) is further divided by 2, because the linear biasing only allows the calculation of the rate Γ over one of the barriers. As opposed to the number of crossing trajectories, which monotonously increases with f_b^{equiv}, the boost factor has a maximum of $B \approx 500$ near

$f_b \approx 1.5$ for the constant bias force, and $B \approx 4000$ near $V_b \approx 0.8$.

Quantitatively the decrease in efficiency can be understood by considering a simple model for the accumulation of $p(t)$ as a function of time t in the linear region of the curve. In calculating the rate Γ, the horizontal axis is divided into n bins of length Δt. In the linear region of length τ, the probability that the crossing occurs at a time belonging to the ith bin is equal for all bins: $p_i = 1/n = \Delta t/\tau$. The probability that any given bin holds m crossing events is therefore binomially distributed, with p_i being the acceptance probability and the number of crossings, N_{cross}, being the number of trials. The problem is analogous to the problem of surface growth by random deposition, with the corresponding quantities being the mean jump rate $\Gamma \triangleq \langle h \rangle$ (average surface height), the standard deviation of mean jump rate $\sigma_\Gamma \triangleq w$ (surface width), $N_{\text{cross}} \triangleq t$ (time), and $n = \tau/\Delta t$ corresponds to the number of lattice sites. For MD, the height of each increment is given by one over the number of trajectories $h = 1/N_{\text{traj}}$. The results for Γ and σ_Γ follow from the well-known results of the random deposition model (see, e.g., Ref. [19]) by direct substitution: $\Gamma = (1/\tau)(N_{\text{cross}}/N_{\text{traj}})$ and $\sigma_\Gamma = (\Gamma/\sqrt{N_{\text{cross}}})\sqrt{1 - 1/n} \approx \Gamma/\sqrt{N_{\text{cross}}}$ for sufficiently large n. For PIHD, on the other hand, the height of the individual increment is not constant, but its distribution can be computed from the distribution of $I_\xi(t_{\text{cross}})$. The probability density $\mathcal{P}(H)$ of having a total increment of H in any one bin i is

$$\mathcal{P}(H) = \sum_{m=1}^{N_{\text{cross}}} \binom{N_{\text{cross}}}{m} p_i^m (1 - p_i)^{N_{\text{cross}}-m} P\left(\sum_{l=1}^{m} h_l = H\right). \qquad (19)$$

The distribution of h_l is approximately log-normal. Since we are not aware of any analytical form for the distribution of the sum of log-normal random variables, the last term in Eq. (19) has been computed numerically. The boost factors according to the random deposition model are shown with the blue markers in Fig. 4. The agreement with the direct measurements from simulations is very good, which indicates that the observed decrease in the boost factor with strong bias is caused by the long-tailed distribution of the weight factors in Eq. (13). This long tail gives large weight for a small minority of trajectories, effectively reducing the number of crossing paths that contribute to the PIHD average. In addition, the systematic error at large bias decreases the boost, because as the bias increases, sufficient sampling of the tail of the distribution $\mathcal{P}(H)$ would require an increasing number of simulated trajectories.

Finally, we note that the maximum boost factor for the sinusoidal bias force is almost ten times larger than the corresponding maximum for the constant bias force. A factor of 2 is explained by the asymmetry of the constant bias force, which effectively eliminates all transitions across the barrier on the left-hand side. In addition, the required constant bias force amplitude to completely remove the barrier on the right is $f_{\text{crit}} = \pi \approx 3.14$, which is much larger than the corresponding equivalent force for the sinusoidal bias: $f_{\text{crit}}^{\text{equiv}} = \frac{\pi}{\sqrt{2}} \approx 2.22$. For high constant bias forces, a large portion of the bias force is effectively wasted in merely shifting the locations of the

minimum and maximum. This is easily seen by looking at the curves in Fig. 1. The sinusoidal bias force, on the other hand, targets the locations of steepest ascent of the potential $V(x)$, giving a significant improvement in the overall boost. This result suggests that an efficient choice of the bias potential is the one that uniformly lowers the activation barrier and preserves the symmetry of the system. By carefully choosing the bias potential, the boost factor of the PIHD method can be significantly improved.

B. Brownian particle in periodic potential with time-varying bias

Diffusion coefficient

In this section, we employ PIHD for parallel resampling of a Brownian particle in a one-dimensional spatially periodic potential with an external, time-dependent ac driving force [2–5]. For such a system, the equation of motion is given by

$$m\ddot{x}(t) + m\gamma\dot{x}(t) - F(x) = \xi(t) + A\sin(2\pi\nu t), \quad (20)$$

where the second term on the right-hand side indicates an ac driving force with amplitude A and frequency ν. The diffusion of a Brownian particle can be studied with respect to various values of these two parameters. Here, we have used the PIHD method to numerically solve Eq. (20) with $A = 0$. The diffusion coefficients for different values of A and ν can be obtained by choosing $F_b(A,\nu) = A\sin(2\pi\nu t)$ and then estimating the functional $I_\xi(t, F_b)$ and the reweighting factor $\exp(-\beta I_\xi)$ for every bias force.

The parameters we have used in the present work are $V_0 = 2$, $T = 1$, $\gamma = 2$, $\lambda = 1$, and $m = 1$. Here we also employed both the BBK and Ermak integration algorithms. We found that the required time step for the BBK algorithm is the same for both PIHD and unbiased MD, while the Ermak algorithm required a shorter time step ($\Delta t = 0.0005$) for high-bias forces (large values of A). At high-bias forces the approximation of the Ermak algorithm becomes insufficient due to the time dependence of the bias force in the product $F_b(x,t)\xi(t)$ of Eq. (7). With the BBK algorithm this problem does not occur.

An interesting issue in Brownian motion under time-periodic forcing concerns the existence of stochastic resonance, which leads to a significant enhancement of the relevant transition rates [5]. In the case of a double-well potential, SR is expected to occur in the vicinity of the matching condition $\nu_r = \Gamma/2$, where Γ is the (thermal) escape rate [5]. Similarly, in the case of an extended periodic potential there is enhancement of local jumps over the barrier V_0 [2]. However, it has been shown in Refs. [2,3,5] that this enhancement exactly cancels out in the hydrodynamic limit for a 1D periodic potential such as used in the present study. One can estimate the resonance frequency ν_r as [5]

$$\nu_r = \frac{\pi V_0}{2\gamma}e^{-V_0}. \quad (21)$$

The calculation results in $\nu_r = 0.213$. Our data for the diffusion coefficients as extracted from the MSD with $A = 0$ using Eq. (10) are shown in Fig. 5. The data have been obtained for a range of values of A ($A = 0.1, 0.5, 1.0, 1.5$) and the frequency ν, and averaged over 10^6 trajectories. We find that for the currently used amplitude values $A \leqslant 1.5$ and frequencies
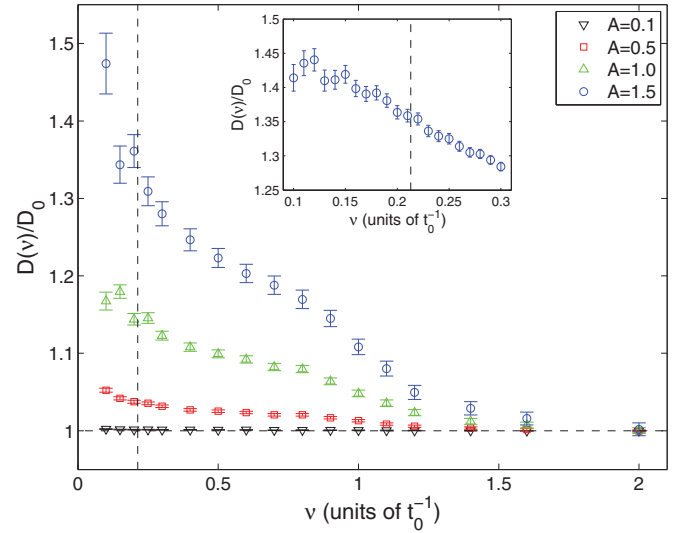

FIG. 5. (Color online) Diffusion coefficients D for the ac-driven Brownian particle in a periodic potential as a function of the driving frequency ν for various values of the amplitude A. The reference value of the diffusion coefficient D_0 (horizontal dashed line) is taken as the value at zero amplitude $A = 0$. The numerical value of D_0 is 0.1570 ± 0.0002. The vertical dashed line indicates the position of the resonance frequency ν_r (see text for details). The inset shows a magnification of higher accuracy data for $A = 1.5$ in the neighborhood of ν_r.

up to $\nu = 30.0$, the diffusion coefficients are monotonically decreasing functions of ν, and there is no stochastic resonance in this system.

The PIHD boost factor

For the parallel resampling the boost factor B can be defined similarly to the barrier crossing problem: B is the ratio of computational time of MD simulations over the computational time of PIHD simulations required to give the same accuracy of the diffusion coefficient D. Here, the difference is that the bias force is not used to accelerate the dynamics, but instead to obtain the diffusion coefficient for multiple values of A and ν while solving the equations of motion just once. Therefore the optimal gain is dependent on the time that is spent on numerically solving the equations motion as compared to computing the correction factor $\exp(-\beta I_\xi)$. Clearly, the simple case of a single particle in an external potential gives an estimate on the minimum boost that can be attained with parallel resampling: with a complex many-particle system the time spent on solving the equations of motion can become very large as compared to calculating the correction factor, and therefore the boost factor can be much higher.

In the present setting of a single particle, a parallel resampling of 100 combinations of A and ν was able to achieve a modest boost factor of $B \approx 2$–3, taking into account the increased noise due to the exponential average (for direct comparison with MD, see Table II). The effect of the noise increases rapidly after $A = 1.5$, which indicates that the parallel resampling of a single particle under ac bias is limited to relatively small bias forces (i.e., low amplitudes A). On the other hand, because increasing the frequency ν of the ac bias

TABLE II. Values of the diffusion coefficient D from PIHD and direct solution of Eq. (20) with $\nu = 0.2$.

A	D [from Eq. (20)]	D (PIHD)
0.1	0.1569 ± 0.0001	0.1570 ± 0.0002
0.5	0.1630 ± 0.0002	0.1631 ± 0.0003
1.0	0.1827 ± 0.0004	0.1825 ± 0.0012
1.5	0.2139 ± 0.0005	0.2162 ± 0.0035

force does not lead to an increase in the action functional $I_\xi(t)$, there are no limits on the extrapolation of ν other than those set by the simulation time and the time step of the underlying MD simulation. In addition, for a system with more degrees of freedom, we expect the boost factor to be much higher due to the increased computational cost of the equations of motion. We also note that at lower temperatures it would be possible to use a static bias potential to boost the number of jumps (cf. preceding section) in combination with parallel resampling for maximal computational boost.

V. CONCLUSION

In this work, we have employed the recently proposed PIHD scheme to study the diffusive motion of Brownian particles in periodic potentials in one dimension. In the first case, we have considered the diffusion of a monomer in the low-temperature and high-friction regime, where we have used the PIHD method to boost the number of jumps across the external potential barrier. We have measured the boost factor (increase in computational efficiency) to reach an optimum of approximately 4000 with the present set of parameters. In addition, we observe a decrease in the boost factor as the bias force is increased beyond the optimal value. This decrease is caused by the exponential averaging of the path sampling and is explained by a simple mathematical model. Intuitively, we can conclude that if the bias force significantly changes the original system, the boost is reduced by the inefficient sampling of the transition paths. For instance, in our benchmark case, the boost starts to decrease as the activation barrier disappears or, when the symmetry of the system is significantly altered.

In the second case, we have demonstrated that the PIHD method can be used to extrapolate results to multiple values of the bias force from a single simulation run. Here, we have used the PIHD method to extrapolate the diffusion coefficient of a monomer moving in a periodic potential under an ac force for multiple values of the ac amplitude and frequency. Our results are in agreement with previous studies and show that there is no stochastic resonance in this system. In this case, the PIHD boost remains modest due to the simplicity of the equation of motion. Finally, we note that the PIHD method is not limited to simple single-particle systems considered in this work. The method can be used even with entropic activation barriers Ref. [11] and, as shown in Ref. [12], it can be easily generalized for systems with internal degrees of freedom, such as polymer chains.

[1] T. Ala Nissila, R. Ferrando, and S. C. Ying, Adv. Phys. **51**, 949 (2002).

[2] J. Kallunki, M. Dubé, and T. Ala Nissila, Surf. Sci. **460**, 39 (2000).

[3] Zhang and Bao, Surf. Sci. **540**, 145 (2003).

[4] L. Y. Chen and P. L. Nash, J. Chem. Phys. **121**, 3984 (2004).

[5] J. Kallunki, M. Dubé, and T. Ala Nissila, J. Phys. Condens. Matter **11**, 9841 (1999).

[6] A. F. Voter, J. Chem. Phys. **106**, 4665 (1997).

[7] D. Hamelberg, J. Mongan, and J. A. McCammon, J. Chem. Phys. **120**, 11919 (2004).

[8] J. C. Wang, S. Pal, and K. A. Fichthorn, Phys. Rev. B **63**, 085403 (2001).

[9] J. A. Rahman and J. C. Tully, J. Chem. Phys. **116**, 8750 (2002).

[10] R. I. Cuckier and M. Morillo, J. Chem. Phys. **123**, 234908 (2005).

[11] L. Y. Chen and N. J. M. Horing, J. Chem. Phys. **126**, 224103 (2007).

[12] J. Shin, T. Ikonen, M. Khandkar, T. Ala Nissila, and W. Sung, J. Chem. Phys. **133**, 184902 (2010).

[13] J. Nummela and I. Andricioaei, Biophys. J. **93**, 3373 (2007).

[14] H. A. Kramers, Physica **7**, 284 (1940).

[15] R. Ferrando, R. Spadacini, and G. E. Tommei, Phys. Rev. E **48**, 2437 (1993).

[16] A. Brünger, L. Brooks III, and M. Karplus, Chem. Phys. Lett. **105**, 495 (1984).

[17] D. L. Ermak and H. Buckholtz, J. Comput. Phys. **35**, 169 (1980).

[18] M. P. Allen and D. J. Tildesley, *Computer Simulation of Liquids* (Clarendon, Oxford, 1994).

[19] A.-L. Arabasi and H. E. Stanley, *Fractal Concepts in Surface Growth* (Cambridge University Press, Cambridge, 1995).